Effect of a stabilizing magnetic field on the electric-field-induced Fréedericksz transition in 4-*n*-pentyl-4-cyanobiphenyl

Shila Garg* and Salman Saeed
Physics Department, College of Wooster, Wooster, Ohio 44691

U. D. Kini
Raman Research Institute, Bangalore 560 080, India
(Received 22 December 1994)

We report an experimental study on electric (**E**)-field-induced static and dynamic distortion of the nematic director in the bend Fréedericksz geometry using electrodes with circular cross sections. In the absence of a stabilizing magnetic (**B**) field, the voltage threshold (V_{th}) for change from the initial homeotropic alignment is different when measured at different points of the sample and is nearly twice the bend threshold; the hysteresis width observed upon reduction of voltage is nearly $V_{th}/2$. The threshold voltage increases with $B=|\mathbf{B}|$ but the static distortion above threshold is periodic with the wave vector in the sample plane being normal to the electrodes (Y stripes) at low B or parallel to the electrodes (X stripes) at high B. On continuous increase of voltage above the Y stripe threshold at constant B, the stripes initially become oblique (XY) and then disappear; subsequent diminution of voltage leads to exhibition of hysteresis with the formation of X stripes. At constant voltage above the Y stripe threshold, an increase of B leads to the appearance of X stripes. Rapid increase of voltage at constant B causes transient XY stripes. Some of the results are qualitatively discussed taking account of the nature of the **E** field.

PACS number(s): 61.30.Gd

I. INTRODUCTION

The director orientation in a nematic sample can be influenced by the application of electric (**E**) and magnetic (**B**) fields leading to transitions between different states of director distortions. Of late, considerable interest has been evoked by the study of the effects of "crossed" **E** and **B** fields on nematic samples, with **E**, **B**, and the initial director orientation $\mathbf{n}_0$ being mutually orthogonal [1]. In nematics with high positive dielectric anisotropy (ε_A), the ac electric-field induced bend Fréedericksz transition in the absence of a stabilizing **B** field is one of the first order [2,3] resulting in a homogeneous deformation above threshold; hysteresis is also observed when **E** is diminished. The first order nature of the transition is theoretically established using the Landau theory [2,3]. In the presence of a strong stabilizing **B** field applied along $\mathbf{n}_0$ for materials with positive diamagnetic susceptibility anisotropy χ_A, however, the static deformation above the transition is periodic with the wave vector of modulation normal to the electrodes [3]. In thick samples subjected to a strong stabilizing **B** field, thermal fluctuations in the director orientation get selectively enhanced parallel to a transverse **E** field, leading to the sample becoming optically biaxial [3].

Two different theoretical explanations have been proposed to account for the modulated structure. In both, the **E** field is assumed to be uniform below the threshold. In the first [4], a simple mathematical model shows that the homogeneous distortion (symmetric about the mid-plane) is unstable against periodic perturbations and that the modulated structure appears above a first order transition. In the second approach [5], it is shown that the unperturbed homeotropic alignment can become unstable against periodic perturbations at a threshold that is lower than the second order Fréedericksz threshold; in this case, the possibility of the modulated structure appearing above a second order transition cannot be ruled out. Interestingly, the predictions of Ref. [5] are in good agreement with experimental observations [3].

Other instances exist where the threshold for periodic distortion is lower than the Fréedericksz threshold. In the splay geometry with a **B** field, a homogeneously aligned sample of a nematic with high elastic anisotropy exhibits a periodic distortion [6] when B exceeds a threshold. Interestingly, when B is increased further, the periodic deformation goes over to a homogeneous one via a first order transition and reappears under decrease of B exhibiting hysteresis [7]. In the same geometry, a periodic deformation occurs in nematics under the action of a dc **E** field [8] due to flexoelectricity [9].

A sudden application of an **E** or a **B** field normal to $\mathbf{n}_0$ leads to the formation of transient periodic structures [10–13]. While in the case of a **B** field [11,12] the periodicity wave vector is along $\mathbf{n}_0$, with an **E** field [13] it may be perpendicular to $\mathbf{n}_0$.

In this paper, we present experimental results on the transitions induced in the director field of a sample of nematic 5CB (4-*n*-pentyl-4′-cyanobiphenyl) subjected to a potential difference parallel to the sample planes in the presence of a stabilizing **B** field. We study the range of existence of the periodic distortion as a function of voltage and B. The choice of 5CB (purchased from EM Industries) is suitable for this investigation as it has high

*Author to whom correspondence should be addressed.

positive ε_A and a positive diamagnetic anisotropy (χ_A); in addition, preliminary investigations on modulated structures were reported using this material [3].

II. EXPERIMENTAL SETUP

The experimental arrangement is shown in Fig. 1. The sample cell is constructed from microscope slides. Thin wires epoxied on the base plate serve as electrodes and spacers yielding a sample thickness ($2h$) of 550 μm. Care is taken to ensure that the spacing between the wires is uniform with the electrode separation ($2g$) being 2.05 mm (Fig. 3) and 4.6 mm (Figs. 4–8); cells with $2g=3.6$ and 3.2 mm have also been used for making preliminary observations on the **E** field effect in the absence of a **B** field. Preparation of different samples is necessitated by the deterioration of alignment, migration of the sealing epoxy material into the cells, etc. Making samples with different g helps explain, in a way, the dependence of threshold on the electrode gap. In earlier work [3], the application of **E** was done somewhat differently using flat metal planes to sandwich the sample. The present arrangement is employed mainly to find out how the **E** field effects are likely to be affected by the shape of the electrodes.

The plates are surface treated with a silane solution (mixture of 3-trimethoxysilyl propyldimethyloctadecyl ammonium chloride, distilled water and isopropyl alcohol) and the induced homeotropic alignment confirmed using conoscopy. Previous experience [14] shows that silane can impart strong homeotropic anchoring at the sample planes. The cell is housed in an aluminum thermostat in which the temperature can be maintained at 28 °C correct to ±1 mK. The thermostat is positioned between the poles of an electromagnet so that the **B** field is normal to the sample planes (along the z axis). A Melles-Griot He-Ne laser of 3 mW power incident normal to the plates is used to initially monitor the Fréedericksz threshold. Observations are made with the polarizer and analyzer crossed at ±45° (in the xy plane) relative to the z axis. The transmitted light intensity is monitored by a photodiode whose output after suitable amplification is fed into a channel of a Keithley 199 digital multimeter. The details of this part of the experiment are similar to those reported earlier [14].

The primary source of voltage is a sinusoidal signal at 1500 Hz from a Hewlett Packard 3325B function generator. The signal is amplified by Kepco BOP 500M bipolar power supply whose output, measured by a channel on the Keithly 199, is applied across the electrodes in the cell after being passed through a high pass filter. In the absence of the nematic liquid crystal, this should produce an **E** field parallel to the x axis near the sample middle ($x=0=z$). In the experiments, the voltage is ramped up at a fixed rate by controlling the output from the signal generator through a GPIB interface and LabView software run on a Macintosh IIci personal computer. The frequency generator has a maximum output of 10 V_{pp} and a resolution of 0.03% over the range used. The gain on the preamplifier of the bipolar power supply is adjustable through an external variable resistor arrangement; in turn, the resistor helps control the maximum value as well as the step size of the applied voltage. The stepping process is closely monitored to minimize electrical noise in the applied voltage. Different ramp rates have been tried; most of the data presented are obtained at a ramp rater of 0.001 V sec^{-1}. A higher ramp rate of 0.34 V sec^{-1} has also been used to induce dynamic changes in the director field.

The current for the electromagnet is supplied by two Kepco ATE 36-30 power supplies connected in series and controlled through a Kepco SN-488 programmer which, in turn, is programmed through an IEEE computer bus system from the Macintosh IIci.

The transition to the modulated phase is investigated wit the setup shown in Fig. 2. An Olympus 8.4 mm industrial fiberscope with a 100° field of view near the focus adaptor tip is snaked through the hole drilled in the pole

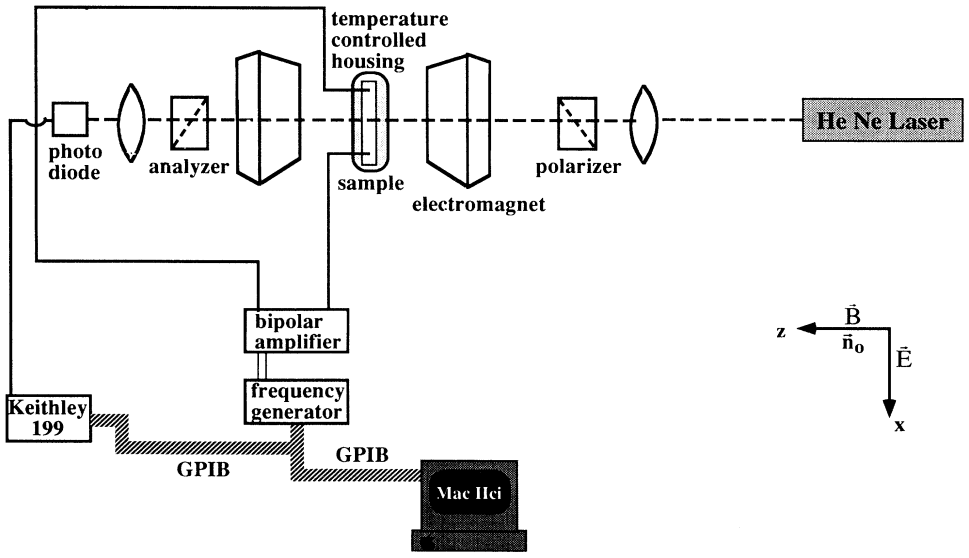

FIG. 1. The experimental block diagram. E: electric field; B: magnetic field; n_0: undistorted director.

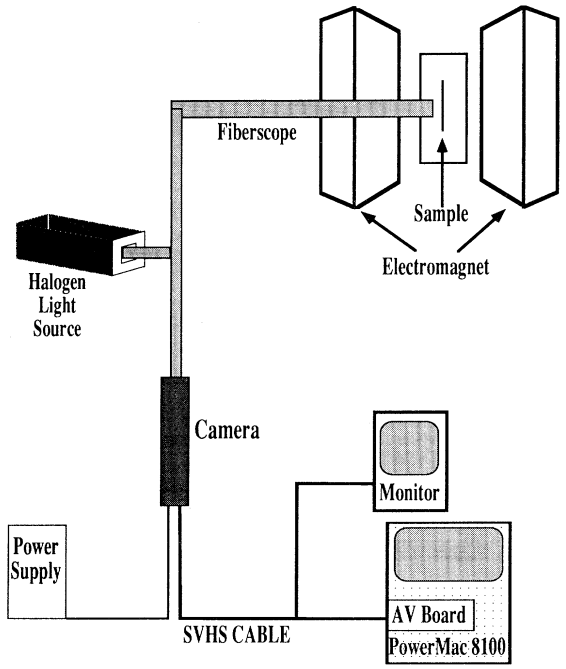

FIG. 2. Experimental arrangement for photographing the periodic phase. (AV, audiovisual; SVHS, supervideo home system.)

of the magnet through which the laser beam is normally passed. The tip can be positioned within 5 mm of the cell and remote controlled in two perpendicular directions (x and y) so that it can be correctly positioned to view the bulk of the sample. The back end illumination is provided by a diffused white light source. The fiberscope is also connected through a "C" mount to a Sony model XC-999 CCD color video camera with 768×494 picture elements ensuring a high resolution image. The output from the camera can be optionally monitored on an 8 in. high resolution color video monitor and recorded onto a videotape on a Panasonic four-head VCR for storing images. Most of the data are obtained by positioning the fiberscope tip near the sample center ($x=0$), midway between the two electrodes. Observations can also be made by taking the tip closer to one of the electrodes and these results are useful in determining the nature of the **E** field inside the sample.

Best results are obtained by directly feeding the camera output into a power Macintosh model 8100 personal computer with an audio-visual board. Then the modulated phase can be observed in real time; images can be recorded at appropriate moments and stored as PICT files. Subsequently, the PICT files can be digitally processed using Adobe PhotoShop software and printed on a LaserPro 630 high resolution printer.

III. OBSERVATIONS OF THE STRIPED PHASE

In the absence of the B field the deformation above threshold is supposed to be homogeneous; this means the distortion is uniform in the sample plane (a function of z alone) and the value of the threshold should be the same regardless of where observations are made. When the voltage is increased from zero, the output from the photodiode initially remains zero. Then the photovoltage starts to increase and finally peaks at $V=V_{\rm th}$ which we regard as the threshold voltage. Above the transition, the director appears to be aligned in the xz plane in a major portion of the sample (as found from optical observations); this is expected for a material with high, positive ε_A. At $B=0, V_{\rm th}$ is found to be 26.44 V_{pp} for observations near the sample center with $2g=3.6$ mm. For observations close to the electrodes, $V_{\rm th}$ is found to be 22.45 V_{pp}, showing that at a voltage for which deformation is not recorded near the sample center, distortion has already set in near the electrodes; this will be shown to be due to the peculiar nature of the **E** field between the two wire electrodes. The dependence of $V_{\rm th}$ on g is, however, as expected. For $2g=3.2$ mm, for instance, $V_{\rm th}=22.1$ V_{pp}. The remaining results are all presented for observations made at $x=0$.

When the voltage is diminished from $V_{\rm th}$ for the $2g=3.2$ mm sample, the photodiode intensity shows a peak at $V'=13.3$ V_{pp}; this corresponds to a considerable change in the director orientation near the sample center; when the voltage is further diminished to $V''=11.02$ V_{pp} (which is nearly $V_{\rm th}/2$), the photodiode intensity goes to zero, showing that the director orientation has become homeotropic at $x=0$. A qualitative interpretation for these observations is given later.

The **E** field induced transition is studied for several B values in the range 0–0.2 T. With a **B** field, the photointensity versus voltage plots reveal varying degrees of fluctuation in the vicinity of the threshold. With increasing B, the threshold also increases. But for a strong **B** field, the distortion above threshold is periodic. Interestingly, however, a plot of threshold voltage versus **B** shows a linear relationship (Fig. 3).

At a sufficiently elevated and constant B, the modulated phase (similar to that reported earlier [3]) can be ob-

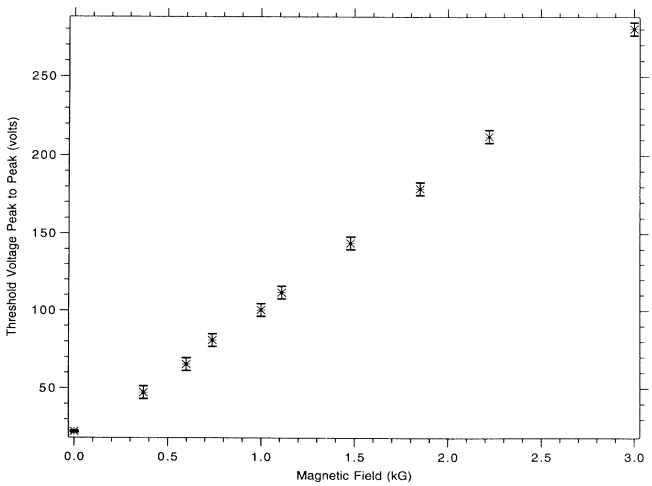

FIG. 3. A plot of threshold voltage ($V_{\rm th}$) versus magnetic field (B), for electrode separation of 2.05 mm.

served when the voltage crosses a threshold V_1. At constant voltage, the stripes (modulations) appear and move across to fill the central region of the cell; the stripes are found to exist for long periods of time. The appearance of the stripes and their movement along x can be recorded in real time as the voltage is increased from zero. The stripes are vertically oriented, parallel to the electrodes (along y) and move from one to the other electrode completely filling the cell; this modulated phase (Y stripes) has its wave vector along x, normal to the electrodes. When the voltage is enhanced further and crosses a second threshold V_2, the stripes start to curl up in the process of disappearing, showing that the Y stripes get tilted in the xy plane when the voltage is increased above V_1; with a further increase of voltage, the cell becomes completely free of stripes. Figures 4(a)–4(d) show the sequence of events as the voltage is increased from 190 V_{pp} to 240 V_{pp} at $B=0.15$ T. At about 238 V_{pp}, the vertical stripes curl up, exhibiting modulation in the xy plane (XY stripes) and also start to dissolve. At a voltage of about 280 V_{pp}, the cell becomes completely clear. A surprising observation is that when the voltage is stepped up fast enough, the xy modulation is dominant compared to the x modulation and the disappearance of the stripes is accompanied by a considerable amount of curling up as seen from Figs. 5(a) and 5(b). We conclude that when the time rate of increase is fast enough, transient features involving XY stripes predominate over the static deformation (Y stripes), which has x modulation.

In the next part of the experiment, observations are continued as the voltage is diminished from 275 V_{pp} with B at 0.15 T. Surprisingly, only weak stripes parallel to x (X stripes with wave vector along y) appear when the voltage is ramped down; the Y stripes are not observed. Figure 6 shows the deformation at 191 V_{pp}. We conclude that when the voltage is decreased from a high value, the Y stripes are unstable relative to X stripes; even the latter are barely visible.

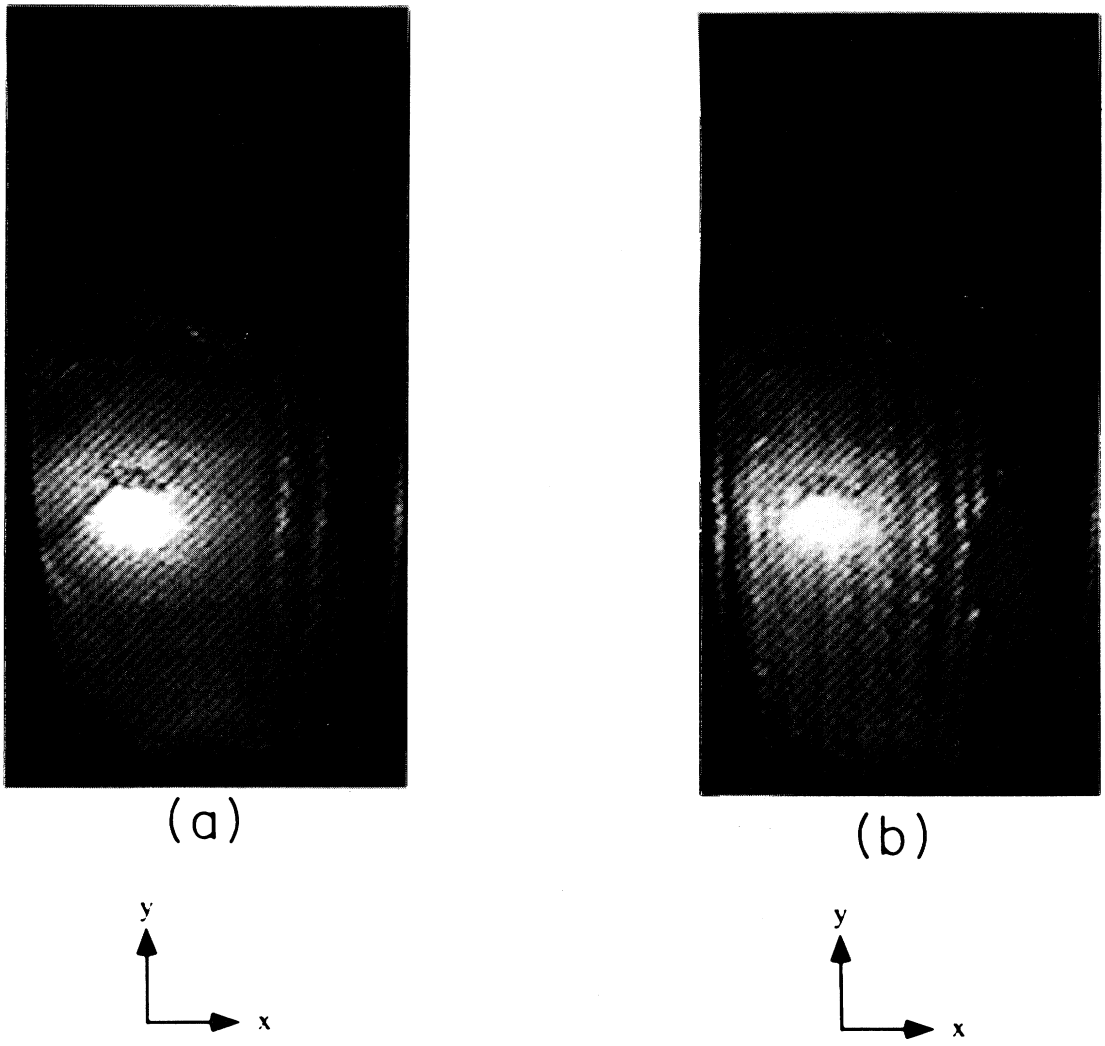

FIG. 4. Sequence of Y stripes appearing, filling up the cell, and disappearing for fixed $\mathbf{B}=0.15$ T as voltage is ramped up from 190 to 240 V_{pp} at a rate of 0.001 V sec.

It is next necessary to explore whether the Y stripes can be recovered after the XY stripes have formed. This is done by increasing the voltage from zero in the presence of a magnetic field until the XY stripes appear. Now, the voltage is slowly diminished. In this experiment, the X stripes form and appear much clearer than in the earlier case; yet, it is not possible to recover the Y stripes through a decrease of voltage after the XY stripes have formed.

So far, B has been held constant and the voltage varied. We now describe results for the reverse case. At $B=0.15$ T, the voltage is stepped up until the Y stripes appear. The voltage is further enhanced and held constant at 228 V_{pp}; B is now increased from 0.15 T. Figure 7 shows the appearance of the cell at 0.162 T. It is found that the stripes take the x orientation under an increase in B.

Mention must be made of the behavior of the distortion when B is very high (0.2 T) and the voltage is ramped up from zero. The deformation above threshold is found to consist predominantly of X stripes; thus, the direction of periodicity which is along x at low B changes to y when the magnetic field is strong enough. Figure 8 shows the appearance of the sample at $B=0.2$ T when the voltage is stepped up quickly. The distortion has periodicity along both x and y and exhibits gridlike features. It may be noted that the deformation reported in earlier literature [3] is indeed periodic along two mutually perpendicular directions in the same plane.

IV. INTERPRETATION OF RESULTS

As a first step toward a theoretical interpretation, consider the case $B=0$. It is known [2,3] that the bend Fréedericksz transition for $B=0$ in 5CB is one of the first order involving hysteresis. As the width of the transition is small, expression (8) of Ref. [5] adequately describes the threshold in terms of relevant parameters including the bend elastic constant K_3. For 5CB parameters [3,15]

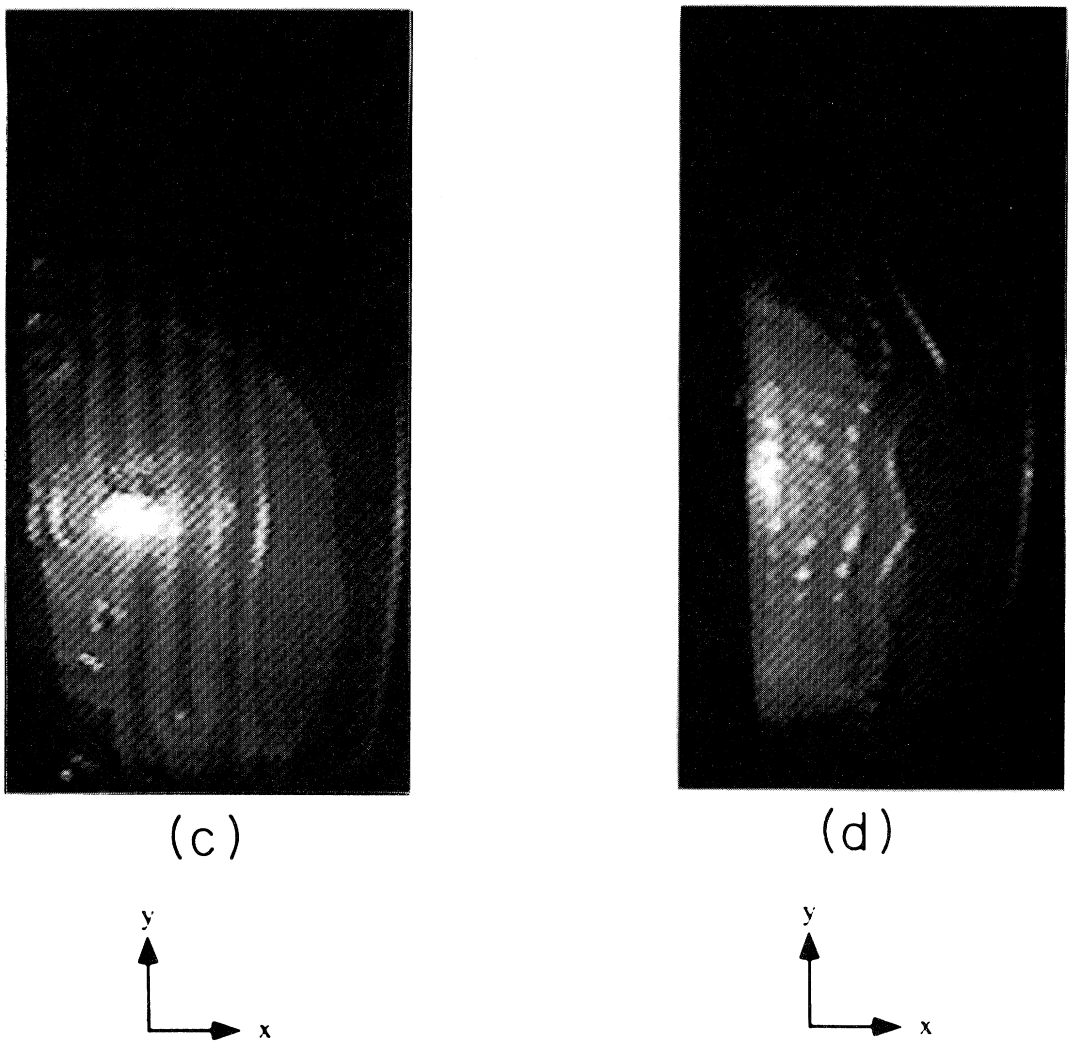

FIG. 4. (*Continued*).

($\varepsilon_{\parallel}=18.8$, $\varepsilon_{\perp}=8.2$, $\chi_A=1.1\times10^{-7}$ emu, $K_3=6.67\times10^{-7}$ dyne; $\varepsilon_{\parallel}$ and $\varepsilon_{\perp}$ are the principal dielectric constants with $\varepsilon_A=\varepsilon_{\parallel}-\varepsilon_{\perp}$); the calculated threshold 11.75 V_{pp} for $2g=3.6$ mm is less than V_{th} by nearly a factor of two. This, coupled with the observation of change in threshold measured at different points between the electrodes, indicates that V_{th} does not correspond to the bend transition above which a uniform director orientation suffers a homogeneous deformation which is symmetric with respect to the sample center ($z=0$); the picture that emerges is the following.

Figure 9 shows a cross section of the sample in the xz plane (not drawn to scale) between $-g\leq x\leq g$ and $-h\leq z\leq h$. 1 and 2 are the glass plates and 3 and 4 the electrodes. In the absence of voltage, the director **n** (represented by thick, short lines) is aligned along z in the sample. Suppose a small voltage is applied between 3 and 4. Since 3 and 4 are conductors, the lines of force will be normal to the surface of 3 and 4. At the sample center (x axis) the line of force (5) will lie along x itself. But at other points (6 and 7), the line of force will curve in the xz plane and will lie parallel to the x axis only exactly midway between the two electrodes, $x=0$. The actual contour of the lines is more complicated, not only close to the electrodes due to the polarization induced in the glass plates but also elsewhere due to the nematic liquid crystal being an anisotropic dielectric; Fig. 9 only serves the purpose of a qualitative interpretation. The **E** field is tilted toward z near the electrodes and its tilt is opposite on either side of the sample center. Hence, **n** gets deformed as shown in regions R_1 and R_3. Writing $\mathbf{n}=(\sin\theta(x,z), 0, \cos\theta(x,z))$, the deformation angle θ is antisymmetric in x at a given z and antisymmetric in z at given x; in particular, $\theta=0$ at $x=0, z=0$; this means **n** midway between the electrodes (in region R_2) will remain homeotropic. Similarly, $\mathbf{E}=(E_x(x,z),0,E_z(x,z))$; while E_x is a symmetric function of x,z, E_z is an antisymmetric function having the same nature as θ. Compared to the deformation above the usual bend transition which is a symmetric function of z and not strongly dependent on x, $\theta(x,z)$ can be regarded as the next higher harmonic; in fact, $\theta(x,z)$ can be regarded as a periodic distortion having a wave-

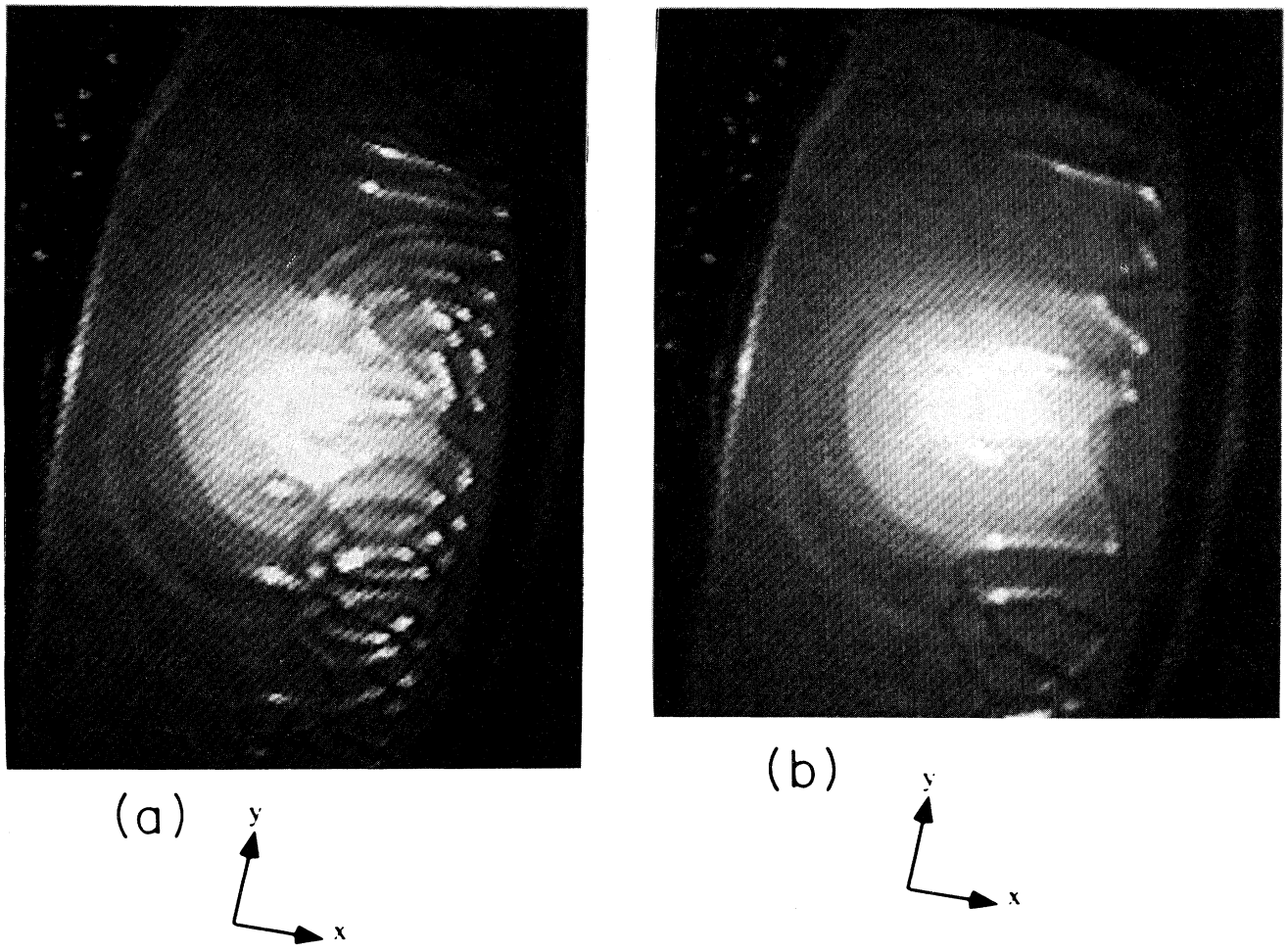

FIG. 5. Appearance of XY stripes with a higher ramp rate of 0.34 V sec.

length of $4g$. When the voltage is increased, the deformation in R_1 and R_3 increases but **n** in R_2 remains homeotropic and, hence, R_2 gets pinched with increased distortion taking place on either side of it. It is possible that this configuration becomes unstable above the threshold V_{th}. The fact that the deformation angle is an antisymmetric function of z suggests, in a way, why V_{th} is nearly twice the expected value of the bend threshold, V_B. Since the theoretical models developed earlier [2–5] assume that **E** in the absence of deformations is uniform, it appears impossible to use them to interpret the results of this work. Since the material has a high, positive ε_A, and since $V_{\text{th}}=2V_{\mathbf{B}}$, we expect that the director field will be of the form $\mathbf{n}=(\sin\phi(z),0,\cos\phi(z))$ in a major portion of the sample, with $\phi(z)$ being a symmetric function of z. Since the voltage is high enough, ϕ will be close to $\pi/2$ in the sample except near the sample planes.

It is not difficult to predict what happens when the voltage is diminished. Once the torque due to the **E** field diminishes, the elastic torque tends to take the director back to the initial configuration. Noting that the **E** field tends to favor the configuration shown in Fig. 9, it is to be expected that when the voltage is diminished sufficiently, the director deformation will go over from the $\phi(z)$ type to the $\theta(x,z)$ type at a lower voltage V''. Since this will involve a considerable change in the overall alignment, it may cause the peak observed in the photodiode intensity at a voltage V' just above V''.

It is natural to expect that with a stabilizing **B** field, V_{th} will increase. We have not yet developed a mathematical model to account for the occurrence of the periodic deformation in the present work; the following qualitative argument can still be presented. It has been

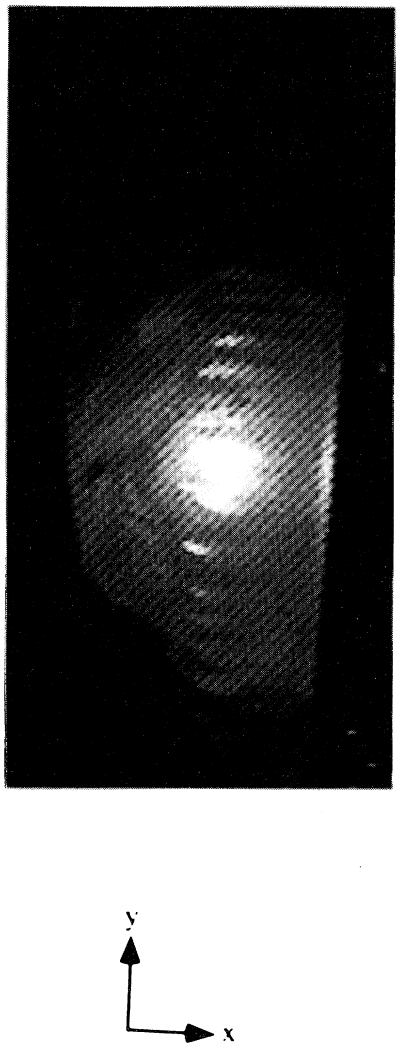

FIG. 6. Appearance of X stripes when voltage is diminished at fixed $\mathbf{B}=0.15$ T.

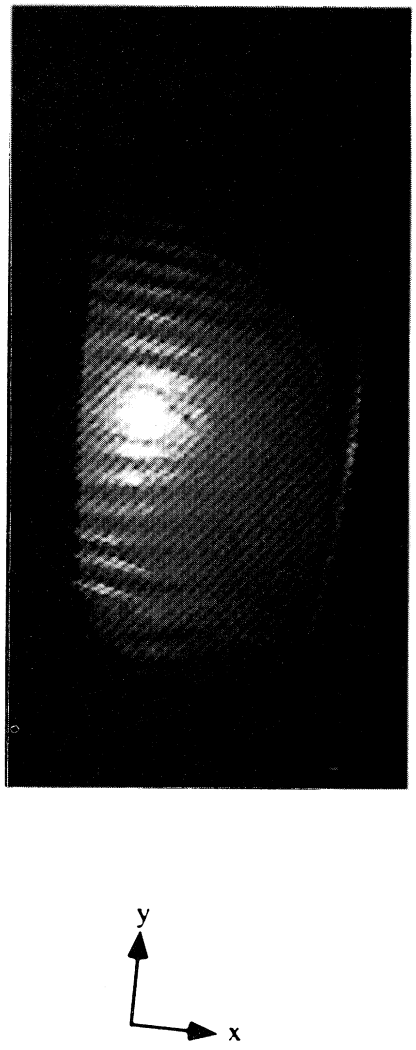

FIG. 7. Appearance of X stripes when voltage is held constant (when y stripes are stable) and **B** field is increased.

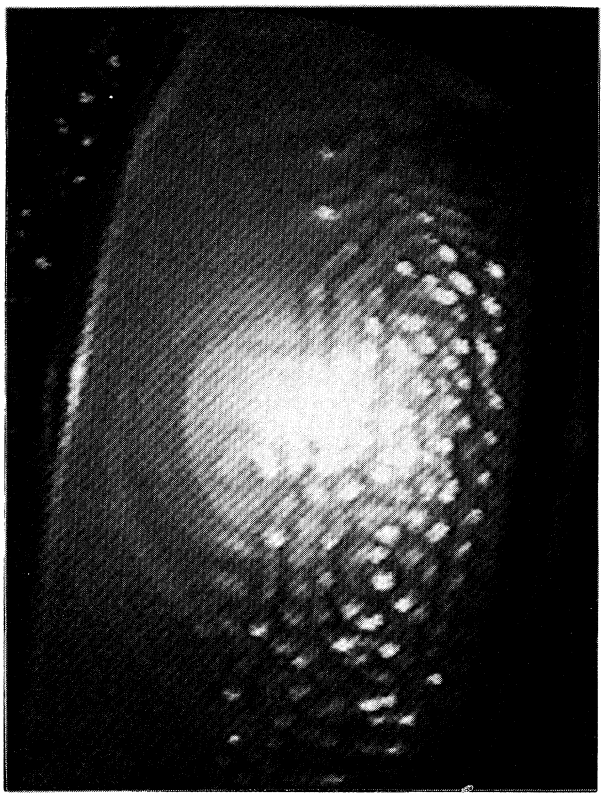

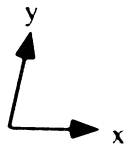

FIG. 8. Gridlike features when voltage is quickly ramped up with a fixed **B** field.

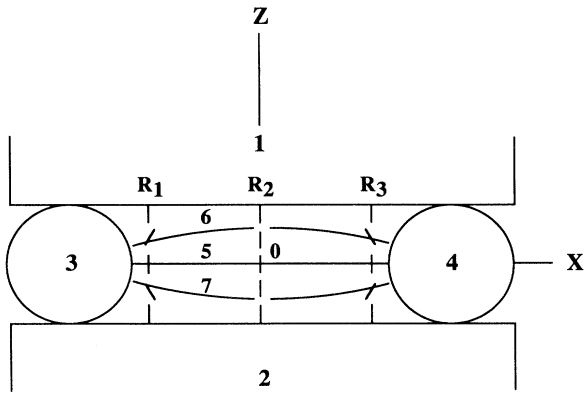

FIG. 9. Cross section of the sample in the xz plane. 1,2: glass plates. 3,4: electrodes. 5: line of force at the sample center. 6,7: lines of force away from the sample center. R_1, R_3: regions of sample close to the two electrodes. R_2: region of sample midway between the two electrodes.

argued earlier [5] that with increasing B in the bend geometry, the destabilizing torques associated with a periodic perturbation can have a stronger influence than that associated with a homogeneous perturbation; this is mainly due to the distortion suffered by the **E** field inside the sample In the present case, it is similarly possible that with increase of B such perturbations in the **E** field cause growth of high wave vector perturbations at a lower threshold.

We have not been able to present here details about the variation of the wavelength of periodicity at threshold for different B. It appears that, in general, the wavelength diminishes with increase in B. For instance, the observed wavelengths at $B=0.169$ and 0.182 T are, respectively, 484 and 379 μm. As a strong **B** field essentially increases the effective K_3 modulus of the sample relative to the other moduli (namely, K_1 and K_2), it is possible to understand intuitively why the periodicity wave vector at threshold increases with B.

Not surprisingly, the theoretical results of Ref. [5] [Eq. (9)] for Y stripes do not agree with those of Fig. 3. For instance, with $B=0.15$ T, the theoretical estimate of the threshold $V_1=51.5$ V_{pp} at 28 °C (including the value of the splay modulus $K_1=5.14$ 10^{-7} dyne) [15] falls well below the experimental value of 120 V_{pp}. We propose to develop a mathematical model to account for our observations.

V. CONCLUSIONS

In conclusion, we have presented experimental observations in the electric-field-induced bend geometry as summarized in the abstract. We have also given a qualitative explanation for some of the observations by analyzing the nature of the **E** field inside the sample. A few points are worth noting. The frequency of voltage used by us is far higher than the viscoelastic frequency associated with a sample of the given thickness. It appears, therefore, that the flexoelectric effect [9] is not important. We propose to repeat these experiments with voltages of different, diminishing frequencies with the hope of studying possible flexoelectric interactions as well as electrohydrodynamic effects [16], which may become important at lower frequencies. Another avenue for investigation is the possible influence of surface anchoring energy and tilt [17] by employing different surface alignment coatings. It is also important to find out how our results will compare with those obtained with plane electrodes [3]. The direction of the **B** field should also play a decisive roll in controlling the features of the instability. It has been shown [5] that the Y stripes may not appear if B is reduced below a limiting value. It is also clear that if the **B** field is applied along x, a periodic instability is unlikely to occur. This leads to the conclusion that for a given B, there must exist a critical tilt of the **B** field away from z at which a static periodic instability may not occur; for a

rapid increase in voltage, a transient periodic instability may still occur. Finally, the possible influence of finite extension of the sample along x (apart from that of electrode shape) must also be considered. This will become clear when parallel experiments using flat electrodes are performed for similar electrode gaps; these studies will be reported in the future.

ACKNOWLEDGMENTS

Partial support was provided to S. G. by the National Science Foundation through Grant No. DMR-8921719. One of us (S.S.) would like to thank the Sophomore Research fund as administered by The College of Wooster.

[1] H. J. Deuling, E. Guyon, and P. Pieranski, Solid State Commun. **15**, 277 (1974); G. Barbero, E. Miraldi, C. Oldano, and P. Taverna Valabrega, Z. Naturforsch. **43a**, 547 (1988).

[2] S. M. Arakelyan, A. S. Karayan, and Yu. S. Chilingaryan, Dok. Akad. Nauk. SSSR **275**, 52 (1984) [Sov. Phys. Dokl. **29**, 202 (1984)].

[3] B. J. Frisken and P. Palffy-Muhoray, Phys. Rev. A **39**, 1513 (1989); B. J. Frisken and P. Palffy-Muhoray, Liq. Cryst. **5**, 623 (1989).

[4] D. W. Allender, B. J. Frisken, and P. Palffy-Muhoray, Liq. Cryst. **5**, 735 (1989).

[5] U. D. Kini, J. Phys. (Paris) **51**, 529 (1990).

[6] F. Lonberg and R. B. Meyer, Phys. Rev. Lett. **55**, 718 (1985).

[7] George Srajer, Frankling Lonberg, and Robert B. Meyer, Phys. Rev. Lett. **67**, 1102 (1991).

[8] L. K. Vistin, Kristallografiya **15**, 594 (1970); Yu. P. Bobylev, V. G. Chigrinov, and S. A. Pikin, J. Phys. (Paris) Colloq. **40**, C3-331 (1979).

[9] R. B. Meyer, Phys. Rev. Lett. **22**, 918 (1969).

[10] E. F. Carr, Mol. Cryst. Liq. Cryst. **34**, L159 (1977).

[11] E. Guyon, R. B. Meyer and J. Salan, Mol. Cryst. Liq. Cryst. **54**, 261 (1979).

[12] G. Srajer, S. Fraden, and R. B. Meyer, Phys. Rev. A **39**, 4828 (1989) (see also references therein).

[13] A. Buka, M. de la Torre Juarez, L. Kramer, and I. Rehberg, Phys. Rev. A **40**, 7427 (1989).

[14] Shila Garg, Karl A. Crandall, and Asad A. Khan, Phys. Rev. E **48**, 1123 (1993).

[15] P. L. Sherrell and D. A. Crellin, J. Phys. (Paris) Colloq. **40**, C3-211 (1979); J. D. Bunning, T. E. Faber, and P. L. Sherrell, J. Phys. **42**, 1175 (1981).

[16] S. A. Pikin, *Structural Transformations in Liquid Crystals* (Gordon and Breach, New York, 1991); L. M. Blinov and V. G. Chigrinov, *Electrooptic Effects in Liquid Crystal Materials* (Springer-Verlag, New York, 1993).

[17] A. Rapini and M. Papoular, J. Phys. (Paris) Colloq. **30**, C4-54 (1969); J. Cognard, Mol. Cryst. Liquid Cryst. Suppl. **1**, 1 (1982).

(c)

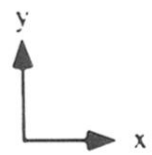

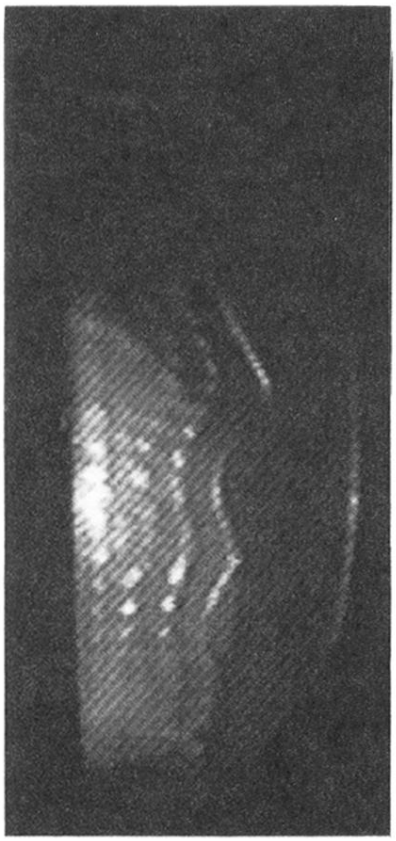

(d)

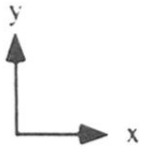

FIG. 4. (*Continued*).

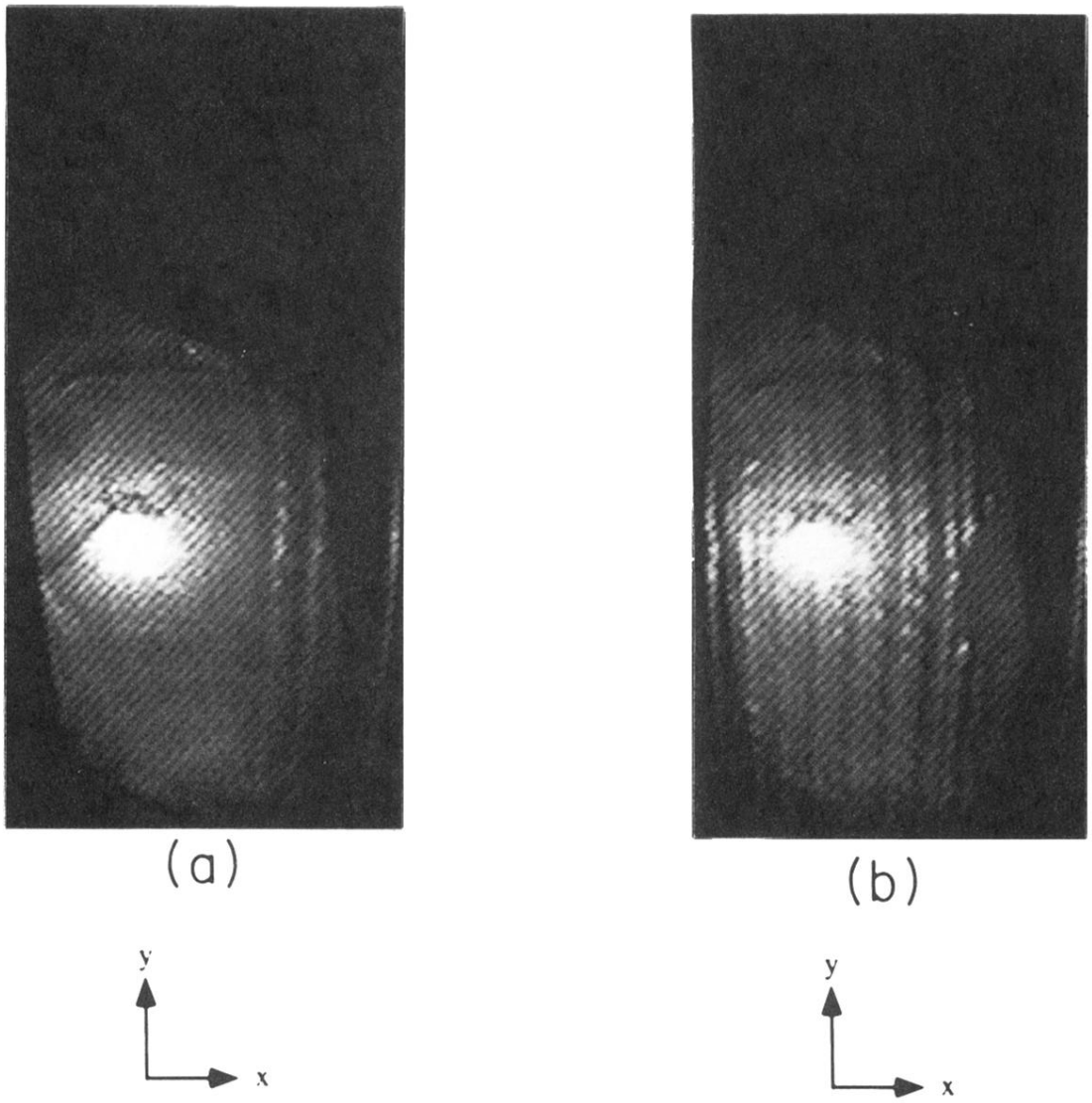

FIG. 4. Sequence of *Y* stripes appearing, filling up the cell, and disappearing for fixed $\mathbf{B}=0.15$ T as voltage is ramped up from 190 to 240 V_{pp} at a rate of 0.001 V sec.

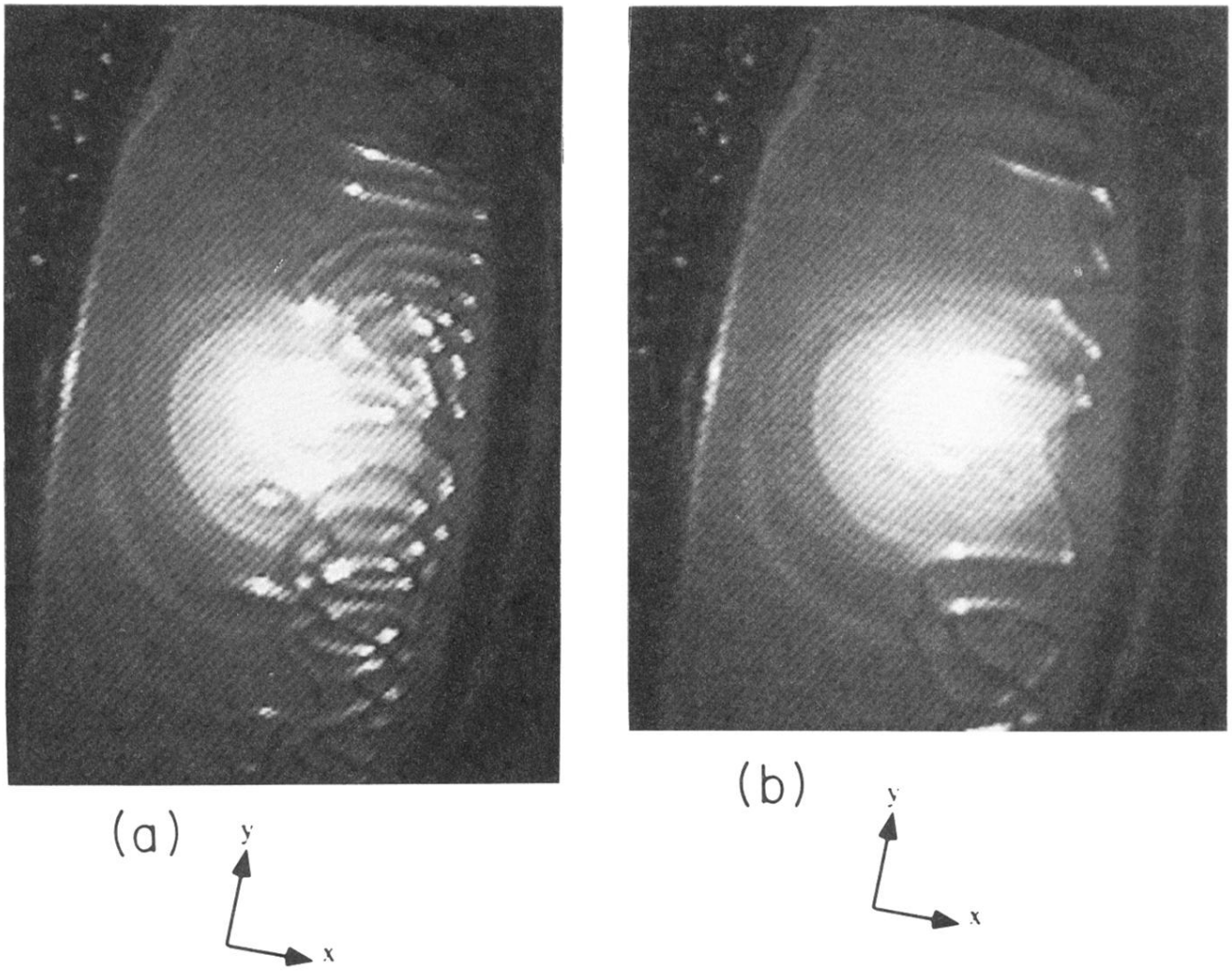

FIG. 5. Appearance of *XY* stripes with a higher ramp rate of 0.34 V sec.

FIG. 6. Appearance of *X* stripes when voltage is diminished at fixed $\mathbf{B}=0.15$ T.

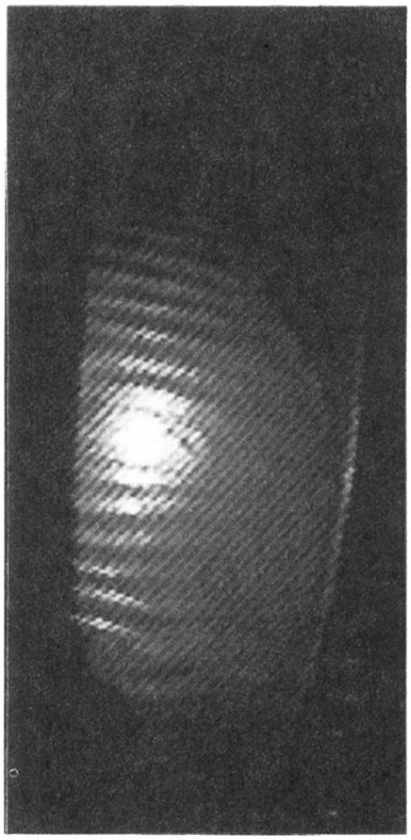

FIG. 7. Appearance of X stripes when voltage is held constant (when y stripes are stable) and **B** field is increased.

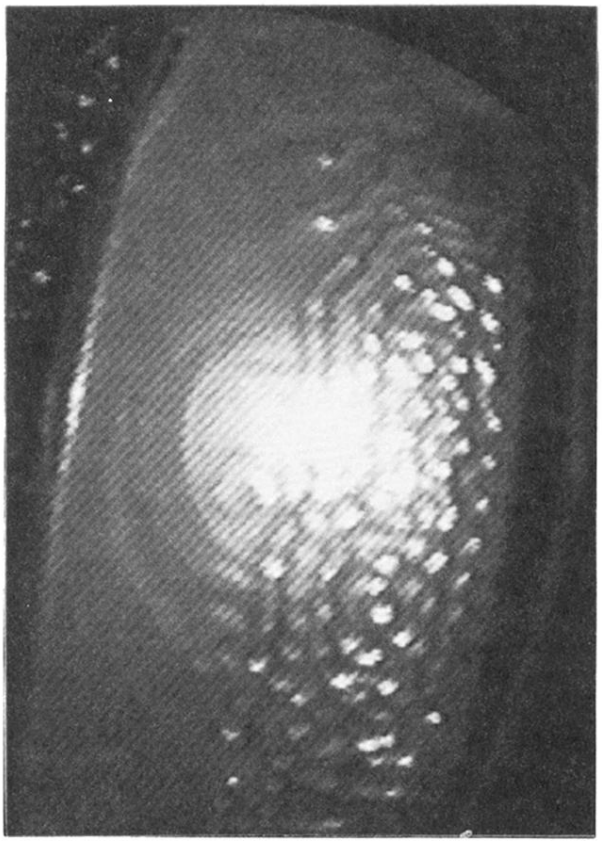

FIG. 8. Gridlike features when voltage is quickly ramped up with a fixed **B** field.